12-18-2019

Is contact nucleation caused by pressure perturbation?

Fan Yang

Will Cantrell

Alexander Kostinski

Raymond Shaw

Andrew M. Vogelmann

atmosphere

MDPI

Article

Is Contact Nucleation Caused by Pressure Perturbation?

Fan Yang [1,*], Will H. Cantrell [2], Alexander B. Kostinski [2], Raymond A. Shaw [2] and Andrew M. Vogelmann [1]

[1] Environmental and Climate Sciences Department, Brookhaven National Laboratory, Upton, NY 11973, USA; vogelmann@bnl.gov

[2] Department of Physics, Michigan Technological University, Houghton, MI 49931, USA; cantrell@mtu.edu (W.H.C.); kostinsk@mtu.edu (A.B.K.); rashaw@mtu.edu (R.A.S.)

* Correspondence: fanyang@bnl.gov

Received: 8 November 2019; Accepted: 13 December 2019; Published: 18 December 2019

Abstract: The reason why ice nucleation is more efficient by contact nucleation than by immersion nucleation has been elusive for over half a century. Six proposed mechanisms are summarized in this study. Among them, the pressure perturbation hypothesis, which arose from recent experiments, can qualitatively explain nearly all existing results relevant to contact nucleation. To explore the plausibility of this hypothesis in a more quantitative fashion and to guide future investigations, this study assessed the magnitude of pressure perturbation needed to cause contact nucleation and the associated spatial scales. The pressure perturbations needed were estimated using measured contact nucleation efficiencies for illite and kaolinite, obtained from previous experiments, and immersion freezing temperatures, obtained from well-established parameterizations. Pressure perturbations were obtained by assuming a constant pressure perturbation or a Gaussian distribution of the pressure perturbation. The magnitudes of the pressure perturbations needed were found to be physically reasonable, being achievable through possible mechanisms, including bubble formation and breakup, Laplace pressure arising from the distorted contact line, and shear. The pressure perturbation hypothesis provides a physically based and experimentally constrainable foundation for parameterizing contact nucleation that may be useful in future cloud-resolving models.

Keywords: ice nucleation; contact nucleation; pressure perturbation

1. Introduction

Ice particles in the atmosphere are important for many cloud processes. For example, growth and sedimentation of ice particles under different environmental conditions can cause various types of surface precipitation, such as snow, hail, and graupel (e.g., [1]). Even for liquid precipitation, a rain drop might have started as an ice particle in the upper atmosphere (e.g., [2]). In addition, ice particles in mixed-phase cloud can absorb extra sunlight and thus reduce surface shortwave irradiance (e.g., [3]). Besides their impacts on precipitation and radiation, ice particles can also create halos by reflecting and refracting sunlight (e.g., [4]). Collision of ice particles in a convective cloud can cause charge separation, and thus lead to cloud electrification and lightning (e.g., [5]). Because of the importance of ice particles to so many processes, it is important to understand the origin of ice particles in atmospheric clouds.

Ice particles in the atmosphere are initially formed through nucleation. Ice nucleation occurs when a thermodynamically stable ice embryo first appears within a metastable liquid drop (supercooled water) or a gas volume (supersaturated water vapor) [6]. At a temperature below ≈ -38 °C, an ice embryo can form spontaneously inside a supercooled water droplet, without the help of an ice nucleating particle (INP), which is called homogeneous ice nucleation [7]. At a higher temperature (between 0 °C and -38 °C), an ice embryo can form with the help of INP, which is called heterogeneous ice nucleation [7]. There are four modes of heterogeneous ice nucleation: deposition, condensation, immersion, and contact. Definitions of the four modes are detailed in Vali et al. [8] and are briefly summarized below. Deposition ice nucleation occurs when an ice embryo forms on the surface of an INP directly through the deposition of water vapor. Condensation ice nucleation occurs when freezing is triggered while an INP is serving as a cloud condensation nucleus. If condensation occurs on an INP and freezing is triggered at some later time (perhaps after the INP is transported into a region with lower temperature), the INP is called an immersion nucleus. Contact ice nucleation occurs when an INP comes into contact with the surface of a supercooled droplet and triggers the freezing. Ice nucleation has been extensively studied in recent decades, and various parameterizations of ice nucleation have been used in cloud models. However, the mechanisms for ice nucleation are still not fully understood at a fundamental level, which limits the realism of ice formation representations in atmospheric models, and thus, might impact weather forecasts and climate projections.

Of the possible nucleation modes, contact ice nucleation is unique for its unusually high efficiency, but has a poorly understood mechanism. For deposition nucleation and immersion nucleation, arguments are made that ice nucleation is initiated at special sites on the surface of INPs (referred to as "active sites" in Fletcher [9]). Although the concept of active sites has been under debate for many years (see Vali et al. [8] and the interactive peer review discussion), recent electron-microscopic observations and high-speed imaging show some evidence that freezing prefers to initiate at specific locations on the surface of an INP, which seems to support the existence of active sites (e.g., [10,11]). However, numerous laboratory experiments since the 1950s have shown that ice nucleation is more likely to occur at a high temperature when an INP makes contact with a water droplet than when the INP is fully immersed in a droplet (e.g., [12–14]), suggesting that contact nucleation is more efficient at a high temperature than immersion nucleation. The mystery is that, if the chemical and/or physical properties of an INP's active sites control the freezing temperature, why is the freezing temperature different (higher) when an INP makes contact with a supercooled drop than when an INP is embedded in the same droplet? Ladino Moreno et al. [15] review experimental studies of contact freezing before 2013 and state, *"There is no complete theory that describes contact freezing"*.

Recent intriguing laboratory experiments have shed light on contact nucleation. For example, Niehaus and Cantrell [16] found that the impact of endothermic or exothermic salt particles with a supercooled drop can initiate freezing. In addition, supercooled drops agitated by either electrowetting [17] or mechanical vibration [18] can freeze at a higher temperature than motionless drops. A candidate explanation for all of these observations is that, besides temperature and the property of an INP, pressure perturbation might be another important variable controlling ice nucleation.

In this paper, we address the following questions: Can pressure perturbation explain previous experiments related to contact nucleation? How large of a pressure perturbation is needed to have a noticeable effect on ice nucleation and to account for the contact nucleation efficiency observed? Is the pressure perturbation realistic and achievable? It should be mentioned that the purpose of this study was not to verify the pressure perturbation hypothesis, because only lab experiments (e.g., directly measuring pressure perturbation during the collision) can verify theory. Instead, we explored the implications of the hypothesis for contact nucleation; specifically, whether the pressure perturbation concept can plausibly explain all existing lab experiments. To answer these questions, we briefly summarize the existing mechanisms used to explain contact nucleation in Section 2. We show that the pressure perturbation hypothesis can explain, qualitatively, all existing lab experiments related to contact nucleation. In order to assess the plausibility of the hypothesis and to guide future experiments and simulations, we considered what pressures are required and on what scales, in order to account for observed contact nucleation efficiencies. Specifically, we estimated the pressure perturbation responsible for contact nucleation caused by the impact of illite or kaolinite. Results are shown in Section 3, and possible atmospheric implications and some suggestions for future experiments are discussed in Section 4.

2. Proposed Mechanisms for Contact Nucleation

2.1. Local Cooling

Knollenberg [19] observed that ice can form when seeding supercooled clouds with urea particles. He argued that this freezing is caused by local cooling due to the dissolution of endothermic salts [20,21]. Compelling evidence for this mechanism is that ice particles are formed in a cloud chamber at temperatures above 0 °C when seeded with urea particles [19]. However, Niehaus and Cantrell [16] found that the impact of exothermic salts with supercooled droplets can also trigger freezing, which cannot be due to local cooling. These salt experiments suggest that local cooling might cause freezing under certain conditions (e.g., [19]), but they cannot explain all the observations related to contact nucleation.

2.2. Etching

Fletcher [22] adapted his previous active site idea [9] and speculated that an active site might be etched when an INP is immersed in a droplet. The etched active site might lose its initial ice nucleation ability, and therefore, immersion nucleation is less efficient than contact nucleation, even for the same INP. He argued that the etching effect might be important for immersion nucleation, and if so, it is important to know the property of active site and the history of its immersion in the cloud droplet. This etching idea suggests an irreversible aspect to contact nucleation, but it is not supported by Shaw et al. [23] in which immersion and contact nucleation can be switched back and forth with no hysteresis or irreversible change.

2.3. Ice Embryo Formed Before Contact

Cooper [24] used classical nucleation theory to describe deposition nucleation and immersion nucleation. His results show that the critical size of an ice embryo for deposition nucleation is about five times larger than that for immersion nucleation. Therefore, an ice embryo formed in the vapor phase might be inactive (smaller than the critical size) for deposition nucleation, but it might be active (larger than the critical size for immersion nucleation) in the liquid, and thus, the impact of such inactive ice embryos with a supercooled water droplet might initiate immersion freezing. Cooper [24] argued that an ice embryo might directly form on an INP from the vapor phase before the INP makes contact with a cloud droplet, and if so, it is important to know the history of the INP within the vapor. Recent modeling (e.g., [25]) and observational (e.g., [26]) evidence shows that ice nucleation might occur more easily in some narrow

regions in porous particles (such as pores, cracks, steps, or capillaries). It is possible that ice embryos can form in porous particles before contact, along the lines of the Cooper hypothesis, but more experiments are needed to verify this explanation. It should be noted; however, that this mechanism is questioned by Fukuta [27] because it can not explain why contact nucleation is more efficient than immersion nucleation.

2.4. Transient Energy Zone During Wetting

Fukuta [28] argued that contact nucleation is due to neither the etching effect, nor an ice embryo being formed before contact. Instead, he proposed that contact nucleation is more efficient than immersion nucleation because a transient energy zone is formed along the surface of an INP during the contact process. Such an energy zone can decrease the energy barrier to the phase change, and thus, benefit nucleation. The formation of the transient energy zone is related to the movement of the water-air interface along the surface of an INP during the wetting process.

2.5. Line Tension

Shaw et al. [23] observed that the freezing temperature is higher when an INP is near the surface of a supercooled drop than when it is immersed in the drop, even without any relative motion. Furthermore, they showed that the change between surface and immersion modes is repeatable. Djikaev and Ruckenstein [29] extended their earlier surface crystallization concept for homogeneous nucleation [30] to include line tensions relevant for heterogeneous nucleation. Sear [31] also found that the nucleation rate at the three-phase contact line is one order of magnitude larger than that inside the bulk liquid, based on an idealized Ising-like model (Potts model). In general, one can argue that the enhancement in ice nucleation rate at the contact line arises from the decrease in energy barrier for phase change due to negative line tension [32].

However, Gurganus et al. [33] and Gurganus et al. [34] did not find a preference for ice nucleation at the contact line for the freezing of a supercooled drop on a silicon substrate. This might be, because, as Sear [31] stated, the volume along the contact line is small compared with the volume inside and therefore, the ice nucleation rate for one drop is still dominated by the bulk property. Interestingly enough, Gurganus et al. [35] observe a preference for nucleation close to the contact line region on a nano-textured optical fiber. They argue that line tension might be important for ice nucleation at the nanometer scale, for which the contribution of line tension to the Gibbs free energy change of phase transition is as important as the contribution of surface tension. Unfortunately, line tension is extremely difficult to measure and the values are poorly known, especially at supercooled temperatures. Winkler et al. [36] estimate a line tension of about -10^{-10} J m^{-1} by measuring the difference between the microscopic contact angle and the macroscopic contact angle (Young angle) at 278 K. If line tension is insensitive to temperature, this suggests that line tension is important for ice nucleation at a length scale of about 1$\sim$10 nm [32].

2.6. Pressure Perturbation

Several recent studies related to contact nucleation cannot be explained by any of the proposed mechanisms above, and the results suggest that pressure might be a cause for freezing. For example, Niehaus and Cantrell [16] found that salt particles, which are not typical INPs because they are water soluble and suppress the freezing temperature, can initiate freezing through impact. Freezing triggered by the impact of exothermic salts rules out the possibility of local cooling suggested by Knollenberg [21]. Niehaus and Cantrell [16] speculate that this freezing might be related to the propagation of a sound wave (pressure wave). Yang et al. [17] found that freezing of supercooled drops on a dielectric film can be initiated by a transient electrowetting field, and that freezing always starts close to the drop perimeter from multiple points. This freezing was shown to be closely related to the distorted contact line due

to electrowetting, rather than the electric field. To completely remove the effect of the electric field, Yang et al. [18] agitated supercooled drops on a vertical oscillating plate, and freezing was observed if the contact line was distorted by either the presence of oil or a substrate with inhomogeneous pinning. Interestingly, high speed videos also show that ice nucleation triggered by electrowetting [17,37] or vibration [18] is strongly related to the distortion and movement of the water-air interface along the surface of the substrate. All three experiments [16–18] were done in isothermal conditions with the temperature much higher than the natural freezing temperature of salts/substrate so that the effect of temperature on ice nucleation could be ruled out. Yang et al. [18] propose that the cause of ice nucleation at high temperatures might be pressure perturbation arising from the impact of salt particles, or the distorted contact line due to either electrowetting or mechanical vibration.

The pressure perturbation hypothesis has at least three merits. First, it is the only mechanism of which we are aware that can plausibly explain nearly all the existing lab experiments related to contact nucleation. For example, a pressure perturbation arising from collision might explain the freezing of supercooled drops due to the impact of INPs (e.g., [15]), salt particles [16], or even another supercooled water drop (first proposed by Hobbs [38], followed by Alkezweeny [39] and Czys [40]). A distorted contact line due to either local inhomogeneous pinning on a rough surface [23,35,41], electrowetting [17], or mechanical vibration [18] might generate a local Laplace pressure perturbation.

$$\Delta p = \frac{2\sigma_w}{r}, \tag{1}$$

where σ_w is the surface tension of water, and Δp is the Laplace pressure inside the liquid due to the distortion of the water surface with a radius of curvature of r. Molecular dynamics calculations have suggested that a nanometer-sized supercooled water droplet will freeze at a temperature much lower than the homogeneous freezing temperature, because its small (positive) radius of curvature leads to a significantly large (positive) Laplace pressure that suppresses ice nucleation [42]. Likewise, it has been speculated based on indirect observations that a small (negative) radius of curvature can lead to a significantly large (negative) Laplace pressure that enhances ice nucleation [18,43]. A quantitative description of how pressure perturbation affects ice nucleation is detailed at the end of this subsection.

Second, the pressure perturbation hypothesis is consistent with the proposed mechanism for ice nucleation induced by acoustic cavitation, for which it is argued that a cavity can be formed through relatively small pressure perturbations due to an acoustic wave. The collapse of the cavity then produces very high positive and then negative pressure amplitudes, which can trigger the freezing of supercooled water [44–46]. Although acoustic techniques have been used to freeze water in the food industry [47,48], their applicability to ice nucleation in the atmosphere is largely unexplored. One recent lab experiment from Schremb et al. [49] found that the impact of a supercooled, degassed water drop on a solid surface had a lower ice nucleation rate compared with the impact of a water drop with a larger gas content, suggesting that ice nucleation might be affected by the bubble generation during the impact. Based on these studies, one could speculate that it is possible for pressure perturbations, resulting from bubble formation (and/or breakup) during the impact of supercooled water droplets with INP, to trigger contact nucleation in the atmosphere.

Third, the pressure perturbation hypothesis has a physical foundation. The ice nucleation barrier of phase transition is quantified by the Gibbs free energy for which temperature and pressure are two fundamental state variables. Therefore, pressure should be the cause of ice nucleation under isothermal conditions. Specifically, the effect of pressure perturbation (Δp) on the change of freezing temperature (ΔT) can be simply expressed as [18],

$$\Delta T = \frac{T_0 \Delta \nu}{l_f} \Delta p, \tag{2}$$

where $T_0 = 273.15$ K, l_f is the latent heat of fusion, and $\Delta \nu = \nu_w - \nu_i$ is the difference of the specific volume between water and ice. Because of the water density anomaly (ice has a larger specific volume than water), a positive pressure perturbation will suppress the freezing temperature. For example, the reason that a nanodroplet will not freeze at a homogeneous freezing temperature might be due to a significantly large positive Laplace pressure arising from a small radius of curvature [42]; equivalently, a negative Laplace pressure perturbation can enhance the freezing temperature [43]. Water at a supercooled temperature and with a negative pressure is called a doubly metastable system [50]. Ice nucleation in "doubly metastable" water has been explored in physics (e.g., [51]), but the connection to contact nucleation has not been established until recently (e.g., [16–18]). It should be mentioned that, besides temperature and pressure, entropy embedded with temperature (see Kostinski and Cantrell [52]) and ice supersaturation ratio as a function of temperature and pressure (see Appendix F in Yang et al. [18]) have also been used to quantify the nucleation process.

3. Estimation of the Pressure Perturbation Responsible for Contact Nucleation

The pressure perturbation hypothesis seems to be a plausible mechanism for contact nucleation; however, it is currently impossible to prove because pressure perturbations relevant to ice nucleation cannot be measured or simulated at such small spatial and temporal scales. In this study, we estimated the pressure perturbation needed to explain previous laboratory results of contact nucleation, assuming that pressure perturbation is the sole cause of freezing. Specifically, we estimated the pressure perturbation needed to trigger ice nucleation through impact with two types of mineral dust, illite or kaolinite, using Equation (2) as the basis for these estimates. We assessed whether the pressure perturbations estimated were realistic and achievable through a comparison with several mechanisms that may produce them.

3.1. Approach

One experimental fact of contact nucleation is that not all impacts of INPs with supercooled water drops can trigger ice nucleation. The contact nucleation efficiency (E) describes how many INP impacts are needed before one freezing event occurs, which can also be interpreted as the probability of ice nucleation for a single collision [15,53]. Another experimental fact is that contact nucleation occurs at a higher temperature compared with immersion nucleation for a given type of INP. So we need to know the immersion freezing temperature of the INPs before we investigate the enhancement due to contact freezing.

The temperature dependence of immersion nucleation is represented using available parameterizations because the mechanism is still unclear at a fundamental level, meaning that we cannot predict from first principles the temperature at which immersion nucleation will occur even if we know the type of INP. The temperature dependence has been observed experimentally for various INPs and parameterized for atmospheric models (e.g., [54]) using either a deterministic or a stochastic approach. The differences and similarities between the two approaches are detailed in several places in the literature (e.g., [55]). Briefly, the deterministic approach (also called the singular approach) is based on experimental observations in which ice nucleation is assumed to depend only on temperature, while the stochastic approach is based on classical nucleation theory in which the ice nucleation rate depends on temperature

and time. The role of time in ice nucleation is still under debate, but it is clear at the moment that ice nucleation is very sensitive to temperature with a lesser sensitivity to time [56].

In this study, we adopt the deterministic approach to quantify the immersion freezing temperature of INP because well-established parameterizations are available that have been verified experimentally. Specifically, the freezing fraction of supercooled drops for a given type of INP at a temperature T is [57],

$$F_{ice,INP} = 1 - \exp\left[-n_{s,INP}(T)A_{INP}\right], \tag{3}$$

where A_{INP} is the total INP surface area inside a droplet, and $n_{s,INP}$ is the surface active site density in units of μm^{-2}. $n_{s,INP}$ is parameterized as a function of temperature for different types of INP based on laboratory experiments [57]. Note that $F_{ice,INP}$ describes the fraction of INP that can trigger immersion nucleation at a certain temperature, which is analogous to the contact nucleation efficiency.

To compute the immersion freezing fractions using Equation (3), A_{INP} is estimated from the contact nucleation experiments described below and $n_{s,INP}$ for each type of INP is obtained from literature. For illite, $n_{s,illite}$ is parameterized based on Broadley et al. [58],

$$n_{s,illite} = \exp\left(A + BT + CT^2 + DT^3\right), T \in \{236.2K \sim 247.5K\}, \tag{4}$$

where $A = 6.53043 \times 10^4$, $B = -8.2153088 \times 10^2$, $C = 3.446885376$, and $D = -4.822268 \times 10^{-3}$. For kaolinite, $n_{s,kaolinite}$ is based on Murray et al. [57],

$$n_{s,kaolinite} = \exp\left(-0.8881T + 226.29\right), T \in \{236.1K \sim 245.5K\}. \tag{5}$$

We also extrapolated n_s to a temperature of 253 K for illite and 258 K for kaolinite, such that the freezing fraction calculated based on Equation (3) covers the lowest values of the measured contact nucleation efficiency. Although the extrapolation follows the rule of thumb that ice nucleation rate/efficiency should be lower at higher temperatures, it is inherently uncertain because of the general lack of direct measurements in the extrapolated range, and thus, it affects our estimation of pressure perturbation in the following section.

Illite is likely one of the best characterized ice nucleating particles explored in the lab at higher temperatures [59]. For comparison, we consider another parameterization equation of n_s for illite based on Hiranuma et al. [60],

$$n_{s,illite} = \exp\left(a\exp\left(-\exp\left(b\left(T + c\right)\right)\right) + d\right), T \in \{-37C \sim -11C\}, \tag{6}$$

where $a = 23.82$, $b = 0.16$, $c = 17.49$, and $d = 1.39$. Note that Equation (6) is the Gumbel cumulative distribution fit to the n_s for the Brunauer-Emmett-Teller (BET) surface area fitted in the linear space of temperature. Parameterization will be different for different fitting strategies (see Table 3 for details in Hiranuma et al. [60]). Kaolinite has fewer data points at higher temperatures, so we chose another parameterization of n_s based on Hartmann et al. [61] for comparison,

$$n_{s,kaolinite} = \exp\left(-0.53T + 6.75\right), T \in \{-37C \sim -32C\}. \tag{7}$$

A detailed discussion of which n_s is more appropriate for extrapolation to high temperatures is beyond the scope of this paper. In this study, we mainly focus on the parameterization of n_s based on Broadley et al. [58] for illite and Murray et al. [57] for kaolinite. Two more parameterizations (Hiranuma et al. [60] for illite and Hartmann et al. [61] for kaolinite) are also considered for comparisons, and their effects on the estimated pressure perturbation are discussed.

3.2. Data

The contact freezing data for illite and kaolinite were measured using the contact ice nucleation chamber described in Niehaus et al. [62]. The illite and kaolinite samples used in that study were from the Clay Minerals Society (https://www.clays.org). Specifically, illite IMT-1 and Kaolinite KGa-2 were used. The materials were used as received, and no further characterizations of the clays were performed. Note that illite and kaolinite samples used in this study were from the same source as those used in Broadley et al. [58] and Murray et al. [57], but they did not have the same size distributions. However, because active site density is normalized by surface area, n_s should have been the same for different sizes of INPs if n_s is scalable. The scalable assumption is widely used in cloud models for simplification, although it has not been verified experimentally. We note that Hartmann et al. [61] reports that differences in assumptions (e.g., geometric vs. BET), methods, or instruments to obtain the surface area can lead to a differences in n_s for kaolinite of more than one order of magnitude.

Illite and kaolinite were aerosolized using a shaken flask, and then the dust was drawn past a droplet that was cooled to the desired temperature on a cold stage. The size distributions measured using a TSI 3330 Optical Particle Sizer are shown in Figure 1. The dust was polydisperse, ranging in diameter from about 1 to 10 μm with a mode at about 2.5 μm. The A_{INP} values used in the immersion freezing fraction calculations (Equation (3)) were estimated from the measured dust size distributions. We used geometric surface area assuming that the particles were spherical. This assumption may be questioned and there are other approaches for determining surface area. For example, the BET method, which estimates surface area by calculating the amount of gas adsorbate on the surface, can yield surface areas that are two times greater than the surface areas derived assuming particles are spheres. In our case, BET measurements were not available, and further, Hartmann et al. [61] confirms that immersion freezing for kaolinite (Fluka) scales with geometric surface area.

Freezing was detected using a diode laser pointing through the test droplet. The transmitted intensity went to nearly zero when the droplets froze because of scattering by the ice. In some cases, the event was verified to be from freezing by removing the top of the sample cell and poking the droplet with tweezers to find that it was solid, verifying that the intensity drop was due to freezing. In some cases, once freezing occurred, the droplets were melted and then cooled back to the original temperature. In those cases, freezing did not reoccur, indicating that the phase transition was triggered by dust impacting the surface, not by deposited dust acting in the immersion mode as, if it was immersion freezing, they should freeze at the same temperature as the initial event.

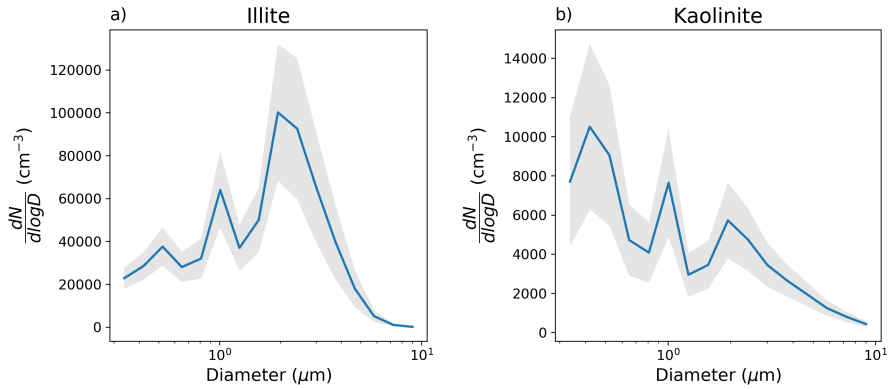

Figure 1. Size distributions of (**a**) illite and (**b**) kaolinite used in contact nucleation experiments [62]. The peak at 1 µm and associated minimum between 1 and 2 µm are artifacts of the sampling setup. The blue line in the figure is the mean, measured over about 30 min of operation. The gray region covers one standard deviation around the mean.

3.3. Results and Discussion

The results in Figure 2 clearly show two observational facts of contact nucleation: (1) the contact freezing temperature (red dots) is higher than the immersion freezing temperature (blue line) for a given efficiency, and (2) not all impacts can trigger contact nucleation. In this study, we wanted to determine the magnitude of the perturbations needed to explain the temperature enhancement over the immersion freezing temperature and the reason for the low contact nucleation efficiency observed, assuming pressure perturbation is the sole cause of contact nucleation. To do so, two extreme assumptions were made to estimate the high and low ranges of pressure perturbations, which are discussed below. It should be mentioned that the pressure perturbation estimated in this study was assumed to be homogeneous inside a droplet for contact nucleation. This assumption was made to simplify the estimation of pressure perturbation. In reality, the pressure perturbation inside the droplet during impact can be both time-dependent and spatially inhomogeneous. The estimated pressure perturbation represents the "effective" pressure perturbation responsible for contact nucleation, rather than a "static" pressure perturbation. In addition, we assumed that the freezing always occurred on the INP that was most recently impacted, and that all INPs were independent from each other. However, it is possible that ice nucleation occurred at a previously impacted (now immersed) INP due to the pressure wave produced by the impacts of subsequent particles. The interaction between the impacted INP and the immersed INP is worth exploring but is beyond the scope of this manuscript. An impact-induced pressure perturbation might also have spatial gradients. This is analogous to the finding that a field of supercooled drops is often not in (metastable) thermodynamic equilibrium [52]. From this gradient perspective, contact nucleation is more favorable than immersion nucleation because the former introduces another sharp gradient at the line of contact. Pressure perturbations can be static as well as dynamic, e.g., wavelike or shear, and those that are dynamic may be more efficient at inducing freezing.

The lower range of the estimated pressure perturbation is obtained by shifting the characteristic immersion freezing curve until it best fits the contact nucleation results. Here, we assumed INPs had a spread of characteristic immersion nucleation temperatures. For example, the majority of illite particles trigger immersion freezing at around −35 °C, while only one out of ten thousand can freeze at around −25 °C. A physical interpretation of the contact nucleation observed in this scenario is that all impacts of INP generate similar pressure perturbations, meaning that the enhancement to the characteristic immersion freezing temperature is the same, and thus, the enhancement can be approximated by a linear

temperature shift in the curve. The low freezing fraction of immersion nucleation at high temperatures is due to rare-but-very-efficient INP, which results in a correspondingly low contact nucleation efficiency. The best-fit curves for illite and kaolinite are shown as the yellow dashed lines in Figure 2. Specifically, the enhancement (shift) of temperature was 4.0 K for illite, corresponding to a pressure perturbation of −44.0 MPa, and it was 9.5 K for kaolinite, corresponding to a pressure perturbation of −104.5 MPa.

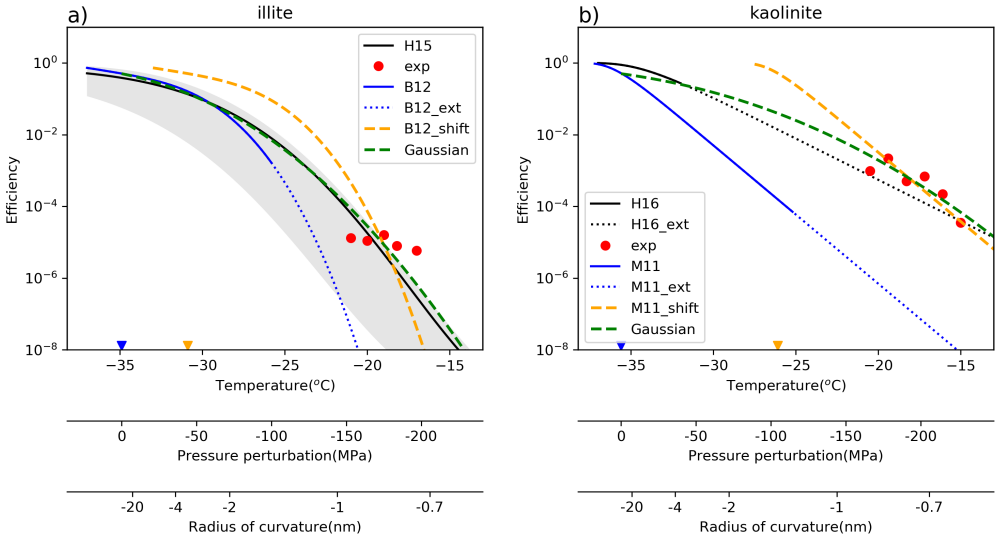

Figure 2. Estimated pressure perturbations needed to account for the measured contact nucleation efficiencies of illite and kaolinite. The red dots are the measured contact nucleation efficiencies, E, where the uncertainty in contact freezing is about a factor of 2∼3. The solid lines are the parameterized immersion freezing fractions calculated based on Equation (3), and the dashed lines are the calculations extended to higher temperatures. Specifically, parameterizations for (**a**) illite were based on (blue) Broadley et al. [58] and (black) Hiranuma et al. [60], while parameterizations for (**b**) kaolinite were based on (blue) Murray et al. [57] and (black) Hartmann et al. [61]. Parameterizations based on Broadley et al. [58] and Murray et al. [57] were used for a basic estimation of the pressure perturbations. The gray region in (a) is the range of uncertainty of n_s for illite reported in Hiranuma et al. [60]. The uncertainties using different parameterizations are discussed in the main text. A lower range of the estimated pressure perturbation is obtained by shifting the (blue) immersion freezing curve to match the measured contact nucleation efficiency, shown as the yellow dashed lines. The horizontal shift is also marked as shift between yellow and blue triangles on temperature axis. A higher range of the estimated pressure perturbation is obtained by adjusting the standard deviation of the pressure perturbation to best match Equation (9) (green dashed lines) with the observed contact nucleation efficiency. The double axes below the temperature coordinate indicate the pressure perturbations responsible for the enhanced temperature relative to the characteristic immersion freezing temperature (marked as blue triangles on temperature axis), and the radius of curvature corresponding a given pressure perturbation.

The higher range was estimated by assuming a distribution of pressure perturbations due to impacts. In this scenario, the same type of INP is assumed to have the same characteristic immersion freezing temperature (T_{INP}). The characteristic freezing temperatures, defined as the temperatures with freezing fractions of 0.5, are −34.9 °C and −35.6 °C for illite and kaolinite. The impact of a large amount of INPs is a distribution of pressure perturbations, and thus a distribution of enhanced freezing temperatures.

A low contact nucleation efficiency arises from rare impact events that cause large pressure perturbations. For simplicity, we assumed a Gaussian distribution of pressure perturbations,

$$f(\Delta p) = \frac{1}{\sqrt{2\pi\sigma_p^2}} \exp\left[-\frac{(\Delta p)^2}{2\sigma_p^2}\right], \tag{8}$$

where σ_p is the standard deviation. For a temperature (T^*) larger than T_{INP}, the enhancement of temperature ($T^* - T_{INP}$) corresponds to a critical pressure perturbation of Δp^*, which can be calculated based on Equation (2). Any impact resulting in a pressure perturbation equal to or larger than Δp^* can trigger ice nucleation at T^*. Therefore, the freezing probability due to one impact (analogous to contact nucleation efficiency) at T^* can be obtained from the error function of the Gaussian distribution of pressure perturbation,

$$F(\Delta p^*) = 1 - \mathrm{erf}\,(\Delta p^*)\,. \tag{9}$$

In Figure 2, σ_p is adjusted to determine the best-fit curve of the computed F with the contact nucleation results, shown by the green dashed line. Specifically, σ_p is -40.7 MPa for illite and -59.4 MPa for kaolinite. Note that the pressure perturbation needed for contact nucleation is much larger than σ_p. It varies from -153 MPa to -197 MPa for illite, and from -166 MPa to -227 MPa for kaolinite.

It should be mentioned that the characteristic freezing temperatures for illite and kaolinite are within the range where homogeneous freezing can be important, suggesting that immersion freezing is not the only process in effect. Only the "best" particles are actually causing immersion freezing above the homogeneous threshold. It is more likely that both the immersion freezing temperature and pressure perturbation vary for different impact events, and the effective pressure perturbation responsible for contact nucleation is between the relatively high and low ranges described above.

When using different parameterizations of n_s (Hiranuma et al. [60] for illite and Hartmann et al. [61] for kaolinite), some inconsistent results were obtained (black lines in Figure 2). The efficiency for immersion nucleation is close to or even larger than that for contact nucleation, meaning that freezing in the experiments of Niehaus et al. [53] is due to immersion nucleation, not contact nucleation. However, this contradicts their hysteresis measurements: they melted and then cooled the drops back to the original freezing temperature but did not observe freezing again at that temperature. The fact that the drops only froze when cooled further is direct evidence that the freezing was catalyzed by contact, not by particles that had hit the droplet and became immersed. The appearance that the efficiency for immersion nucleation is larger than that for contact nucleation is, therefore, inconsistent with the experiments and is unphysical. This was likely a result of the uncertainties in n_s and the surface area obtained from different types and sizes of INPs, and different instruments and methods. One conclusion we might draw from the comparison is that the lower bound of pressure perturbation can be close to 0.

An important question is whether a pressure perturbation of $0\sim-200$ MPa is achievable. It is hard to know the answer at this moment, because we can neither measure nor simulate pressure perturbations at such small temporal and spatial scales. However, interestingly enough, Marcolli [43] shows that the estimated lower range of pressure perturbation (0 to -50 MPa) is realistic in supercooled water, while the higher range (~-200 MPa) is close to the cavitation pressure for homogeneous bubble nucleation. Another question is, if achievable, how might such high negative pressure perturbations be obtained? Here, we propose three possible ways. First, a pressure perturbation might be due to bubble formation and breakup [44–46]. Schremb et al. [49] showed that impact-induced bubbles might serve as additional nucleation sites, and thus enhance the nucleation rate. Second, a pressure perturbation might arise from a large Laplace pressure due to the small radius of curvature. This can be achieved by distorting the contact line through to the impact of INPs (e.g., the neck region), inhomogeneous pinning on a rough

fiber [35], electrowetting [17], or mechanical vibration [18]. The radius of curvature corresponding to the pressure perturbation is also shown in Figure 2. Results show that a nanometer scale of radius of curvature is needed to have a Laplace pressure that is effective at triggering contact nucleation. Last, the pressure perturbation might be related to other components of the stress tensor; e.g., shear. In fact, shear is another type of pressure and is responsible for the deformation of fluid. Results from molecular dynamic simulations show that freezing can be accelerated by oscillatory shear [63].

4. Conclusions and Suggestions

We summarized six proposed mechanisms to explain the long-standing mystery of contact nucleation. Among them, the pressure perturbation hypothesis based on recent experiments can explain nearly all existing results related to contact nucleation. In addition, the pressure perturbation hypothesis has a physical foundation and might be useful for developing physical-based and experimental-constrainable parameterization for contact nucleation. Two mineral dusts, illite and kaolinite, were chosen to estimate the pressure perturbations needed to account for their contact nucleation rates, due to their well-known behavior of immersion nucleation and contact nucleation. Estimated higher and lower ranges were obtained by assuming a Gaussian distribution of pressure perturbation and a constant pressure perturbation. The estimated pressure perturbation is very sensitive, for which parameterization equation of n_s was used. To obtain a best fit to the observed contact nucleation efficiencies, a pressure perturbation would be between -44.0 MPa and -197.0 MPa for illite (corresponding to -3.3 nm to -0.7 nm radius of curvature for achieving the Laplace pressures) based on Broadley et al. [58], and between -104.5 MPa and -227.0 MPa for kaolinite (corresponding to -1.4 nm to -0.6 nm radius of curvature for achieving the Laplace pressures) based on Murray et al. [57]. However, when using other parameterization equations for n_s (Hiranuma et al. [60] for illite and Hartmann et al. [61] for kaolinite), the efficiency for immersion nucleation is very close to that for the measured contact nucleation (although, as discussed, this seems inconsistent with the hysteresis experiments). We cannot provide accurate limits of the estimated pressure perturbations due to the uncertainties of n_s and surface area, but it is safe to say that the absolute value of the pressure perturbation can be as small as 0 Pa and as large as the cavitation pressure, leading to, respectively, a negligible or significant enhancement of the freezing temperature. Three possible approaches are proposed to reach the negative pressure perturbations, including bubble formation and breakup, Laplace pressure arising from the distorted contact line, and shear.

More lab experiments and numerical simulations are needed to evaluate the pressure perturbation hypothesis and quantify its effect on ice nucleation. Here, we provide several suggestions for people who aim to investigate contact nucleation in the future.

- It is important to measure the corresponding immersion nucleation temperature for each contact nucleation event. This will provide the actual immersion freezing temperature for each contact nucleation event, based on direct measurements rather than indirect estimations using the parameterization equations. It can be accomplished by melting ice after contact freezing and then slightly decreasing temperature until immersion nucleation occurs. A superhydrophobic substrate might be used to avoid substrate freezing in cold stage experiments.
- It will be useful to perform contact nucleation experiments for a broader range of temperatures, such that the contact nucleation efficiency varies from 10^{-1} to 10^{-6}. This will extend our understanding of the behavior of contact nucleation and also benefit parameterizations of contact nucleation in cloud-resolving models.
- It will be a major breakthrough if pressure perturbation can be precisely measured or controlled. Experiments such as that in Bird et al. [64], in which the neck region arising from the coalescence

of two droplets was well controlled and quantified, might be useful for investigating the effect of negative Laplace pressures on ice nucleation.

- Numerical simulation might be another useful tool with which to investigate the pressure perturbation hypothesis. If indeed pressure perturbation is a valid mechanism for inducing freezing, then it may be possible to have freezing just through droplet-droplet collisions or droplet breakup. A multi-phase fluid model has been applied to simulate the development of pressure perturbation in the neck region for two collided droplets [65]. The next step is to find a way to realistically simulate the collision process, instead of setting up the neck region initially as in Bartlett et al. [65].

Author Contributions: Conceptualization, F.Y., A.B.K., and R.A.S.; methodology, F.Y., W.H.C., and R.A.S.; writing, F.Y., W.H.C., A.B.K., R.A.S., and A.M.V. All authors have read and agreed to the published version of the manuscript.

Funding: F.Y. and A.M.V. were supported by the US Department of Energy (DOE) under contract DE-SC0012704. W.H.C. was supported by NSF grant number AGS-1541998. A.B.K. was supported by NSF grant number AGS-1639868. W.H.C. and R.A.S. were supported by Department of Energy under contract DE-SC0018931.

Acknowledgments: We are grateful to two anonymous reviewers for their helpful comments and feedback.

Conflicts of Interest: The authors declare no conflict of interest.

References

1. Kikuchi, K.; Kameda, T.; Higuchi, K.; Yamashita, A.; Working Group Members for New Classification of Snow Crystals. A global classification of snow crystals, ice crystals, and solid precipitation based on observations from middle latitudes to polar regions. *Atmos. Res.* **2013**, *132*, 460–472. [CrossRef]
2. Braham, R.R., Jr. Meteorological bases for precipitation development. *Bull. Am. Meteorol. Soc.* **1968**, *49*, 343–353. [CrossRef]
3. Lubin, D.; Vogelmann, A.M. The influence of mixed-phase clouds on surface shortwave irradiance during the Arctic spring. *J. Geophys. Res. Atmos.* **2011**, *116*. [CrossRef]
4. Macke, A. Scattering of light by polyhedral ice crystals. *Appl. Opt.* **1993**, *32*, 2780–2788. [CrossRef] [PubMed]
5. Gaskell, W.; Illingworth, A. Charge transfer accompanying individual collisions between ice particles and its role in thunderstorm electrification. *Q. J. R. Meteorol. Soc.* **1980**, *106*, 841–854. [CrossRef]
6. Lamb, D.; Verlinde, J. *Physics and Chemistry of Clouds*; Cambridge University Press: Cambridge, UK, 2011. [CrossRef]
7. Cantrell, W.; Heymsfield, A. Production of ice in tropospheric clouds: A review. *Bull. Am. Meteorol. Soc.* **2005**, *86*, 795–808. [CrossRef]
8. Vali, G.; DeMott, P.; Möhler, O.; Whale, T. A proposal for ice nucleation terminology. *Atmos. Chem. Phys.* **2015**, *15*, 10263–10270. [CrossRef]
9. Fletcher, N. Active sites and ice crystal nucleation. *J. Atmos. Sci.* **1969**, *26*, 1266–1271. [CrossRef]
10. Kiselev, A.; Bachmann, F.; Pedevilla, P.; Cox, S.J.; Michaelides, A.; Gerthsen, D.; Leisner, T. Active sites in heterogeneous ice nucleation—The example of K-rich feldspars. *Science* **2017**, *355*, 367–371. [CrossRef]
11. Holden, M.A.; Whale, T.F.; Tarn, M.D.; O'Sullivan, D.; Walshaw, R.D.; Murray, B.J.; Meldrum, F.C.; Christenson, H.K. High-speed imaging of ice nucleation in water proves the existence of active sites. *Sci. Adv.* **2019**, *5*, eaav4316. [CrossRef]
12. Rau, W. Unterkühlbarkeit des Wassers und atmosphärische Eisbildung. *Wetter Klima* **1949**, *2*, 81–92.
13. Gokhale, N.R.; Goold, J. Droplet freezing by surface nucleation. *J. Appl. Meteorol.* **1968**, *7*, 870–874. [CrossRef]
14. Gokhale, N.R.; Lewinter, O. Microcinematographic studies of contact nucleation. *J. Appl. Meteorol.* **1971**, *10*, 469–473. [CrossRef]
15. Ladino Moreno, L.A.; Stetzer, O.; Lohmann, U. Contact freezing: A review of experimental studies. *Atmos. Chem. Phys.* **2013**, *13*, 9745–9769. [CrossRef]
16. Niehaus, J.; Cantrell, W. Contact freezing of water by salts. *J. Phys. Chem. Lett.* **2015**, *6*, 3490–3495. [CrossRef]

17. Yang, F.; Shaw, R.A.; Gurganus, C.W.; Chong, S.K.; Yap, Y.K. Ice nucleation at the contact line triggered by transient electrowetting fields. *Appl. Phys. Lett.* **2015**, *107*, 264101. [CrossRef]
18. Yang, F.; Cruikshank, O.; He, W.; Kostinski, A.; Shaw, R.A. Nonthermal ice nucleation observed at distorted contact lines of supercooled water drops. *Phys. Rev. E* **2018**, *97*, 023103. [CrossRef]
19. Knollenberg, R.G. Urea as an ice nucleant for supercooled clouds. *J. Atmos. Sci.* **1966**, *23*, 197–201. [CrossRef]
20. Knollenberg, R.G. A laboratory study of the local cooling resulting from the dissolution of soluble ice nuclei having endothermic heats of solution. *J. Atmos. Sci.* **1969**, *26*, 115–124. [CrossRef]
21. Knollenberg, R.G. The local cooling ice nucleation model. *J. Atmos. Sci.* **1969**, *26*, 125–129. [CrossRef]
22. Fletcher, N. On contact nucleation. *J. Atmos. Sci.* **1970**, *27*, 1098–1099. [CrossRef]
23. Shaw, R.A.; Durant, A.J.; Mi, Y. Heterogeneous surface crystallization observed in undercooled water. *J. Phys. Chem. B* **2005**, *109*, 9865–9868. [CrossRef] [PubMed]
24. Cooper, W.A. A possible mechanism for contact nucleation. *J. Atmos. Sci.* **1974**, *31*, 1832–1837. [CrossRef]
25. Page, A.J.; Sear, R.P. Heterogeneous nucleation in and out of pores. *Phys. Rev. Lett.* **2006**, *97*, 065701. [CrossRef]
26. David, R.O.; Marcolli, C.; Fahrni, J.; Qiu, Y.; Sirkin, Y.A.P.; Molinero, V.; Mahrt, F.; Brühwiler, D.; Lohmann, U.; Kanji, Z.A. Pore condensation and freezing is responsible for ice formation below water saturation for porous particles. *Proc. Natl. Acad. Sci. USA* **2019**, *116*, 8184–8189. [CrossRef]
27. Fukuta, N. Comments on "A possible mechanism for contact nucleation". *J. Atmos. Sci.* **1975**, *32*, 2371–2373. [CrossRef]
28. Fukuta, N. A study of the mechanism of contact ice nucleation. *J. Atmos. Sci.* **1975**, *32*, 1597–1603. [CrossRef]
29. Djikaev, Y.; Ruckenstein, E. Thermodynamics of heterogeneous crystal nucleation in contact and immersion modes. *J. Phys. Chem. A* **2008**, *112*, 11677–11687. [CrossRef]
30. Djikaev, Y.; Tabazadeh, A.; Hamill, P.; Reiss, H. Thermodynamic conditions for the surface-stimulated crystallization of atmospheric droplets. *J. Phys. Chem. A* **2002**, *106*, 10247–10253. [CrossRef]
31. Sear, R.P. Nucleation at contact lines where fluid–fluid interfaces meet solid surfaces. *J. Phys. Condens Matter* **2007**, *19*, 466106. [CrossRef]
32. Gurganus, C. Investigating the Role of the Contact Line in Heterogeneous Nucleation with High Speed Imaging. Ph.D. Thesis, Michigan Technological University, Houghton, MI, USA, 2014.
33. Gurganus, C.; Kostinski, A.B.; Shaw, R.A. Fast imaging of freezing drops: No preference for nucleation at the contact line. *J. Phys. Chem. Lett.* **2011**, *2*, 1449–1454. [CrossRef]
34. Gurganus, C.; Kostinski, A.B.; Shaw, R.A. High-speed imaging of freezing drops: Still no preference for the contact line. *J. Phys. Chem. C* **2013**, *117*, 6195–6200. [CrossRef]
35. Gurganus, C.; Charnawskas, J.; Kostinski, A.; Shaw, R. Nucleation at the contact line observed on nanotextured surfaces. *Phys. Rev. Lett.* **2014**, *113*, 235701. [CrossRef]
36. Winkler, P.; McGraw, R.; Bauer, P.; Rentenberger, C.; Wagner, P. Direct determination of three-phase contact line properties on nearly molecular scale. *Sci. Rep.* **2016**, *6*, 26111. [CrossRef] [PubMed]
37. Hans, R.P. The effect of an external electric field on the supercooling of water drops. *J. Geophys. Res.* **1963**, *68*, 4463–4474. [CrossRef]
38. Hobbs, P. The aggregation of ice particles in clouds and fogs at low temperatures. *J. Atmos. Sci.* **1965**, *22*, 296–300. [CrossRef]
39. Alkezweeny, A. Freezing of supercooled water droplets due to collision. *J. Appl. Meteorol.* **1969**, *8*, 994–995. [CrossRef]
40. Czys, R.R. Ice initiation by collision-freezing in warm-based cumuli. *J. Appl. Meteorol.* **1989**, *28*, 1098–1104. [CrossRef]
41. Durant, A.J.; Shaw, R.A. Evaporation freezing by contact nucleation inside-out. *Geophys. Res. Lett.* **2005**, *32*. [CrossRef]
42. Li, T.; Donadio, D.; Galli, G. Ice nucleation at the nanoscale probes no man's land of water. *Nat. Commun.* **2013**, *4*, 1887. [CrossRef]
43. Marcolli, C. Ice nucleation triggered by negative pressure. *Sci. Rep.* **2017**, *7*, 16634. [CrossRef] [PubMed]

44. Hickling, R. Nucleation of freezing by cavity collapse and its relation to cavitation damage. *Nature* **1965**, *206*, 915–917. [CrossRef]
45. Hunt, J.; Jackson, K. Nucleation of the solid phase by cavitation in an undercooled liquid which expands on freezing. *Nature* **1966**, *211*, 1080–1081. [CrossRef]
46. Hunt, J.; Jackson, K. Nucleation of solid in an undercooled liquid by cavitation. *J. Appl. Phys.* **1966**, *37*, 254–257. [CrossRef]
47. Li, B.; Sun, D.W. Novel methods for rapid freezing and thawing of foods—A review. *J. Food Eng.* **2002**, *54*, 175–182. [CrossRef]
48. Cheng, X.; Zhang, M.; Xu, B.; Adhikari, B.; Sun, J. The principles of ultrasound and its application in freezing related processes of food materials: A review. *Ultrason. Sonochem.* **2015**, *27*, 576–585. [CrossRef]
49. Schremb, M.; Roisman, I.V.; Tropea, C. Transient effects in ice nucleation of a water drop impacting onto a cold substrate. *Phys. Rev. E* **2017**, *95*, 022805. [CrossRef]
50. Pallares, G.; Azouzi, M.E.M.; González, M.A.; Aragones, J.L.; Abascal, J.L.; Valeriani, C.; Caupin, F. Anomalies in bulk supercooled water at negative pressure. *Proc. Natl. Acad. Sci. USA* **2014**, *111*, 7936–7941. [CrossRef]
51. Barrow, M.S.; Williams, P.R.; Chan, H.H.; Dore, J.C.; Bellissent-Funel, M.C. Studies of cavitation and ice nucleation in 'doubly-metastable' water: Time-lapse photography and neutron diffraction. *Phys. Chem. Chem. Phys.* **2012**, *14*, 13255–13261. [CrossRef]
52. Kostinski, A.; Cantrell, W. Entropic aspects of supercooled droplet freezing. *J. Atmos. Sci.* **2008**, *65*, 2961–2971. [CrossRef]
53. Niehaus, J.; Becker, J.G.; Kostinski, A.; Cantrell, W. Laboratory measurements of contact freezing by dust and bacteria at temperatures of mixed-phase clouds. *J. Atmos. Sci.* **2014**, *71*, 3659–3667. [CrossRef]
54. Murray, B.; O'sullivan, D.; Atkinson, J.; Webb, M. Ice nucleation by particles immersed in supercooled cloud droplets. *Chem. Soc. Rev.* **2012**, *41*, 6519–6554. [CrossRef] [PubMed]
55. Niedermeier, D.; Shaw, R.; Hartmann, S.; Wex, H.; Clauss, T.; Voigtländer, J.; Stratmann, F. Heterogeneous ice nucleation: Exploring the transition from stochastic to singular freezing behavior. *Atmos. Chem. Phys.* **2011**, *11*, 8767–8775. [CrossRef]
56. Ervens, B.; Feingold, G. Sensitivities of immersion freezing: Reconciling classical nucleation theory and deterministic expressions. *Geophys. Res. Lett.* **2013**, *40*, 3320–3324. [CrossRef]
57. Murray, B.J.; Broadley, S.; Wilson, T.; Atkinson, J.; Wills, R. Heterogeneous freezing of water droplets containing kaolinite particles. *Atmos. Chem. Phys.* **2011**, *11*, 4191–4207. [CrossRef]
58. Broadley, S.; Murray, B.; Herbert, R.; Atkinson, J.; Dobbie, S.; Malkin, T.; Condliffe, E.; Neve, L. Immersion mode heterogeneous ice nucleation by an illite rich powder representative of atmospheric mineral dust. *Atmos. Chem. Phys.* **2012**, *12*, 287–307. [CrossRef]
59. DeMott, P.J.; Möhler, O.; Cziczo, D.J.; Hiranuma, N.; Petters, M.D.; Petters, S.S.; Belosi, F.; Bingemer, H.G.; Brooks, S.D.; Budke, C.; et al. The Fifth International Workshop on Ice Nucleation phase 2 (FIN-02): laboratory intercomparison of ice nucleation measurements. *Atmos. Meas. Tech.* **2018**, *11*, 6231–6257. [CrossRef]
60. Hiranuma, N.; Augustin-Bauditz, S.; Bingemer, H.; Budke, C.; Curtius, J.; Danielczok, A.; Diehl, K.; Dreischmeier, K.; Ebert, M.; Frank, F.; et al. A comprehensive laboratory study on the immersion freezing behavior of illite NX particles: A comparison of 17 ice nucleation measurement techniques. *Atmos. Chem. Phys.* **2015**, *15*, 2489–2518. [CrossRef]
61. Hartmann, S.; Wex, H.; Clauss, T.; Augustin-Bauditz, S.; Niedermeier, D.; Rösch, M.; Stratmann, F. Immersion freezing of kaolinite: Scaling with particle surface area. *J. Atmos. Sci.* **2016**, *73*, 263–278. [CrossRef]
62. Niehaus, J.; Bunker, K.W.; China, S.; Kostinski, A.; Mazzoleni, C.; Cantrell, W. A technique to measure ice nuclei in the contact mode. *J. Atmos. Ocean. Technol.* **2014**, *31*, 913–922. [CrossRef]
63. Borzsák, I.; Cummings, P.T. Electrofreezing of water in molecular dynamics simulation accelerated by oscillatory shear. *Phys. Rev. E* **1997**, *56*, R6279. [CrossRef]

64. Bird, J.C.; Ristenpart, W.D.; Belmonte, A.; Stone, H.A. Critical angle for electrically driven coalescence of two conical droplets. *Phys. Rev. Lett.* **2009**, *103*, 164502. [CrossRef] [PubMed]
65. Bartlett, C.T.; Généro, G.A.; Bird, J.C. Coalescence and break-up of nearly inviscid conical droplets. *J. Fluid Mech.* **2015**, *763*, 369–385. [CrossRef]